Published in final edited form as:
Ann Biomed Eng. 2013 October ; 41(10): 2099–2108. doi:10.1007/s10439-013-0809-3.

MRI-Apparent Localized Deformation of the Median Nerve Within the Carpal Tunnel During Functional Hand Loading

Jessica E. Goetz[1,2], **Nicole M. Kunze**[1], **Erin K. Main**[1], **Daniel R. Thedens**[3], **Thomas E. Baer**[1], **Ericka A. Lawler**[1], and **Thomas D. Brown**[1,2]

[1]Department of Orthopaedics and Rehabilitation, University of Iowa, 200 Hawkins Drive, 01008 JPP, Iowa City, IA 52242, USA

[2]Department of Biomedical Engineering, University of Iowa, 1402 Seamans Center, Iowa City, IA 52242, USA

[3]Department of Radiology, University of Iowa, 200 Hawkins Drive, 3970 JPP, Iowa City, IA 52242, USA

Abstract

In MR images, the median nerve of carpal tunnel syndrome (CTS) patients frequently appears flatter than in healthy subjects. The purpose of this work was to develop a metric to quantify localized median nerve deformation rather than global nerve flattening, the hypothesis being that localized median nerve deformation would be elevated in CTS patients. Twelve patients with CTS and 12 matched normals underwent MRI scanning in eight isometrically loaded hand conditions. 2D cross sections of the proximal and distal tunnel were analyzed for nerve cross sectional area, flattening ratio, and a position shift to the dorsal side of the tunnel. Additionally, new metrics based on the angulation of the nerve perimeter in 0.5-mm lengths around the boundary were calculated. The localized deformation metrics were able to detect differences between CTS patients and healthy subjects that could not be appreciated from the flattening ratio. During most hand activities, normal subjects had a higher average percentage of locally deformed nerve boundary than did CTS patients, despite having a rounder overall shape. Less local nerve deformation in the CTS patient group resulting from its interaction with flexor tendons suggests that the nerve may be less compliant in CTS patients.

Keywords

Carpal tunnel syndrome; Magnetic resonance imaging; Shape measures; Impingement

INTRODUCTION

Carpal tunnel syndrome (CTS), the most commonly encountered peripheral compressive nerve disorder, is caused by mechanical insult of the median nerve as it passes through the carpal tunnel. Symptoms range from numbness and paresthesia (tingling) in mild cases, to loss of dexterity and muscle atrophy in more severe cases. Development of CTS has often been associated with ergonomic and workplace risk factors. However, the actual mechanism

Address correspondence to Jessica E. Goetz, Department of Orthopaedics and Rehabilitation, University of Iowa, 200 Hawkins Drive, 01008 JPP, Iowa City, IA 52242, USA. jes-sica-goetz@uiowa.edu.

CONFLICT OF INTEREST

This work was funded by National Institutes of Health Grant AR053899. No benefits in any form have been or will be received from a commercial party related directly or indirectly to the subject of this manuscript.

responsible for median nerve insult remains unknown. Diagnosis is typically made based on the results of clinical exam, and supported by electrodiagnostic testing.[7] In equivocal cases, ultrasound or magnetic resonance imaging (MRI) may be used to help confirm the diagnosis.

MRI, with its excellent resolution of the carpal tunnel soft tissues, has long been utilized to catalog various anatomic features in both normal volunteers and cadaveric preparations, in order to identify pathological changes associated with CTS.[10,11,14] Four characteristics associated with CTS have been identified in these types of structure/shape studies: enlargement of the median nerve, flattening of the median nerve, bowing of the transverse carpal ligament, and increased signal intensity of the median nerve on T2-weighted images.[5,11,12,23,24] Unfortunately, despite being frequently identified in patients with CTS, these MRI-apparent anatomic abnormalities are relatively non-specific and insensitive for making the diagnosis.[17,21]

One reason these traditional MRI characteristics have been diagnostically inadequate may be that the changes being reported are very general variations in tissue appearance. For example, the most frequently applied metric for evaluating median nerve shape is the nerve flattening ratio, computed as aspect ratio of an ellipse fit to the nerve boundary. Normally, the nerve appears moderately flattened within the confines of the carpal tunnel, with an average flattening ratio of 2.9 at the hook of the hamate (a perfect circle has a flattening ratio of 1).[10] Unfortunately, while some studies have found that CTS patients have significant nerve flattening (flattening ratio of 3.8),[11] others have found no significant differences between CTS patients and normal subjects.[14] It is plausible that the flattening ratio is simply too insensitive to capture the subtle changes in shape of the frequently non-ovoid median nerve.[25]

A slightly more specific measure, referred to as circularity, has more recently been used to describe median nerve shape. In this context, circularity is defined as the nerve perimeter squared, divided by the quantity 4π times the nerve cross sectional area.[13,22] However, the clinical utility of this shape metric remains unclear, as it too has been shown to discriminate between CTS patients and normals in some cases, but not in others.[22] This metric may be limited due to approximating the median nerve cross section as a smooth, regular shape.

The cross sectional profile of the median nerve frequently includes localized depressions or protrusions due to its interaction(s) with the neighboring flexor tendons and/or the carpal tunnel boundary. These features cannot be captured with low-order global metrics such as flattening ratio or circularity. Yet, it is these localized deformations of the median nerve boundary that seemingly would be a characteristic of contact/insult from neighboring anatomic structures. The goal of this work was to quantify localized deformations in the median nerve boundary and to determine if there were more such occurrences in patients with a history of CTS.

MATERIALS AND METHODS

Acquisition of MRI Scans

Twenty-four subjects (10 male, 14 female) participated in this IRB-approved study, and each participant provided written consent prior to their imaging session. Twelve subjects were selected for study based on both clinical and electrophysiologic evidence of CTS. Clinically, these patients had been diagnosed with CTS after being evaluated by a fellowship-trained hand and upper extremity orthopedic specialist. Patients complained of paresthesias of varying intensity in the median nerve distribution and exhibited positive provocative testing of the median nerve. Based on the clinical evaluation, electrodiagnostic

testing was performed and severity was classified according to the electrodiagnostic testing criteria established by the American Association of Neuromuscular & Electro-diagnostic Medicine: Severe—absence of sensory response and abnormal distal motor latency, Moderate—abnormal sensory distal latency and decreased sensory amplitude, Mild—prolonged sensory distal latency.[6,15] Additionally, patients with normal sensory distal latency but decreased sensory conduction velocity were classified as mild, and in cases where motor latency was affected with normal sensory studies, the patient was classified as a moderate. CTS patients had an average age of 48.4 years (range 29–67) with an average body mass index of 29.9 (range 20.3–40.3), and no history of diabetes, hypothyroidism, inflammatory arthritis, alcohol abuse, metabolic peripheral neuropathy, chronic renal failure, shoulder pathology, or chronic back pain. Two participants had electrodiagnostically mild CTS, five participants were classified as moderate, and five were classified as severe. Despite electrodiagnostic classification, all subjects were quite symptomatic, requiring carpal tunnel release surgery for treatment.

A normal subject who had no history of hand or wrist pathology was matched to each CTS patient by being within 2 years of the patient's age, within 2″ of the patient's height, and within 30 pounds of the patient's weight. Normal subjects also had no history of diabetes, hypothyroidism, inflammatory arthritis, alcohol abuse, metabolic peripheral neuropathy, chronic renal failure, shoulder pathology, or chronic back pain, and each verbally confirmed that they had not experienced CTS symptoms in their scanned hand. No electrodiagnostic testing was performed on the normal study participants. The symptomatic hand, which in all but one case coincided with the dominant hand, was scanned for the CTS patients. The dominant hand was scanned for all normal subjects.

Three-dimensional MR images of each subject were acquired on a Siemens TIM Trio 3T scanner (Siemens Medical, Malvern, PA, USA) using a 90-s dual echo steady state (DESS) pulse sequence (TR/TE = 13.0/4.3 ms). The acquired resolution was 0.2 mm × 0.2 mm × 1.0 mm voxels over an 8 cm × 6 cm × 7.5 cm field of view. Eight different wrist position/loading activity combinations were studied for each subject, and all scans were collected over the course of a single 1-h imaging session. Scans were acquired while the subject (i) relaxed with fingers extended, (ii) performed an isometric four-finger volar flat press (17 N load), (iii) performed an isometric power grip (32 N load), and (iv) performed an isometric index–thumb pulp pinch (6.5 N load) (Fig. 1). Each isometric loading activity was controlled using a custom-built device made of non-ferromagnetic materials. Resistance in the grip device was provided by a length of compressible hollow rubber tubing, and resistance in the pinch and press activities was provided by flexure of polymer sheets. Each device was equipped to provide audio feedback (a beep) to the subject once the correct load was applied, and subjects were instructed to keep the beep constant for the duration of each scan.

For the first four scans, the wrist was stabilized in 0 degrees of wrist flexion (neutral) with a polymeric splint applied to the dorsal aspect of the hand. Splinting on the dorsal side of the hand prevented the splint from artificially compressing the carpal tunnel tissue structures. After the four neutral scans, the subject's wrist was splinted in 35 degrees of flexion, and the four loading conditions were repeated. Subjects were scanned in the prone position, with the arm extended overhead (a "superman" position). A transmit/receive lower extremity coil was used for imaging because it provided the clearance necessary to accommodate both flexed and straight wrist angles plus the isometric loading devices used during the acquisition of functionally loaded scans. Due to motion artifact degradation of the quality of several of the isometrically loaded scans, 19 of the 192 (24 × 8) image series needed to be omitted, leaving a total of 173 image series for analysis.

Image Analysis

The carpal tunnel, median nerve, and digital flexor tendon boundaries were segmented from each MRI volume using a set of custom Matlab (The Mathworks, Natick, MA, USA) programs.[8] Segmentation was initialized by manually tracing the structures on the proximal-most image of the carpal tunnel (i.e., at the level of the proximal pisiform). The segmentation propagated distally using a Chan-Vese active contouring algorithm[3] followed by visual checking and manual editing of the automatically-generated tissue boundaries. Once segmentation was completed, tendon identities (i.e., the finger to which each tendon was directed) were tracked from a distal image within the MRI volume (where tendon identities were unambiguous) back through the carpal tunnel segmentations using a custom-written region growing algorithm.[9] The distal radius and ulna were manually segmented from each scan, and all segmentation data (bony contours plus carpal tunnel tissue segmentations) were rotated into a subject-specific anatomic coordinate system that was defined for each subject using their distal forearm bones. Left hand data was mirrored to yield a right-handed coordinate system for all specimens that was centered at the middle of the radial plateau, with the *x*-axis directed toward the ulnar styloid, the *y*-axis directed volarly, and the *z*-axis directed distally through the shaft of the radius. Referencing all soft tissue data to a bone-based coordinate system afforded consistent orientation of carpal tunnel structure geometries collected when the subjects' arms were in various orientations within the scanner, which was necessary to accommodate the different wrist angulations and functional activities that were imaged. 2D cross sections perpendicular to the carpal tunnel at the levels of the pisiform (proximal tunnel) and the hook of the hamate (distal tunnel) were digitally isolated from the anatomically oriented 3D carpal tunnel models for purposes of performing detailed shape analysis.

Shape Measure Calculations

Median nerve cross sectional area was calculated from the 2D sections at both the proximal and distal carpal tunnel locations using a routine developed in Matlab. The median nerve flattening ratio was computed as the ratio of the major to minor axes of an ellipse fit to the median nerve boundary by the Matlab routine. Mobility of the median nerve was manually indexed based upon the occurrence of a location shift from the nerve's ventral location when the hand was unloaded, to a more dorsal location within the carpal tunnel (Fig. 2). If no shift occurred, a mobility value of 0 was assigned, and if a complete shift to the dorsal side of the tunnel occurred, a value of 1 was assigned. Instances in which the median nerve appeared to be partially shifted and confined by the neighboring flexor tendons were assigned a mobility value of 0.5.

To provide information about localized median nerve deformations, new metrics were developed based on the calculation of shape numbers.[2] First, the Matlab program automatically discretized the perimeter of the median nerve into 0.5 mm line segments, and the interior angle between each pair of adjacent discretized segments was calculated. Shape numbers ranging from −8 to +8 were assigned to each boundary segment by binning each interior angle using 20° slope change increments (Fig. 3). A smoothly elliptical boundary with no abrupt local boundary deformations was typically comprised of low positive shape numbers (0–2), whereas higher shape numbers (closer to 8) indicated a more pronounced outward curvature, or a protrusion, distorting the shape of a boundary from a smooth ellipse. Negative shape numbers indicated an intrusion, defined as a portion of the nerve boundary which was compressed inward toward the center of the structure.

Shape number chains were compiled by concatenating adjacent shape numbers in a clockwise direction around a tissue structure's boundary, starting from the point on the nerve boundary closest to either the pisiform (proximal tunnel) or to the hook of the hamate

(distal tunnel). Severe local distortions in the nerve boundary were considered to be locations where the shape numbers were either negative (intrusion upon the nerve boundary) or ≥3 (pronounced protrusion of the nerve boundary). Nerve perimeter lengths were similarly variable within the normal subject group (average 15.9 mm; SD 2.5 mm) and in the CTS patient group (average 16.4 mm; SD 2.6 mm). Using the 0.5 mm equal-length line segments, the number of deformations was converted to a deformed boundary length, which was normalized to the nerve perimeter, yielding a percentage of locally deformed nerve boundary.

Statistical Analysis

Traditional shape measures (cross sectional area and flattening ratio), plus the occurrence of a dorsal shift within the tunnel, and the new measure of percentage of locally deformed nerve boundary were compared between the CTS patients and the matched normals. Changes in traditional and new shape measures between unloaded and isometrically loaded hand conditions were also identified in each group. Differences between the groups were identified using paired Wilcoxon signed rank tests to account for the low sample numbers and the non-normal distribution of data. All statistical tests were run using GraphPad Prism 5.0 (GraphPad Software, La Jolla, CA, USA), with $p < 0.05$ considered statistically significant.

RESULTS

Nerve Appearance in the Distal Tunnel (Hook of Hamate Level)

In the distal carpal tunnel, regardless of hand activity, flattening ratios were very similar between CTS patients and matched normals, with a non-significant trend of CTS patients having a flatter nerve than normal subjects (Fig. 4). The cross sectional area of the nerve was also very similar between groups, with slight (non-significant) trend of CTS patients having a larger nerve cross section for all activities except the squeeze grip. The normal subjects had a higher percentage of locally deformed median nerve boundary when the wrist was in neutral, regardless of loading activity. However this trend approached statistical significance ($p = 0.055$) only when the hand was in the relaxed neutral configuration (Fig. 5). Normal subjects also had a more mobile nerve than did CTS patients, as indicated by the increase in dorsal shifts in the normal patients as compared to the CTS patients. Again, however, this trend approached statistical significance only when the hand was unloaded ($p = 0.072$).

When the wrist was flexed, the nerve also tended to be flatter in CTS patients than in normal subjects. Nerve cross sectional area while the wrist was flexed was similar between normals and CTS patients across all hand loading conditions. Unlike in the neutral wrist position, in wrist flexion the percentage of the nerve boundary that was locally deformed varied by hand activity. When the hand was relaxed and during the index pinch activity, local deformation was similar between the two groups, whereas during the flat-press activity, there was more localized deformation in the CTS patient group than in the normals (Fig. 5). During the squeeze grip, the normal subjects had more localized deformation. When the wrist was flexed, the nerve was more mobile in the normal patients, demonstrating statistically significantly more dorsal shifting than in CTS patients only during the relaxed-hand ($p = 0.07$) condition.

Nerve Appearance in the Proximal Tunnel (Pisiform Level)

In the proximal part of the tunnel, the morphological trends were very similar to those seen in the distal tunnel. Again, when the wrist was in neutral, CTS patients had slightly flatter and slightly larger nerves than matched normals, and again there was more local

deformation in the normal group than in the CTS patients (p value range: 0.019–0.349). At this proximal tunnel location, the nerve was more mobile in normal subjects than in CTS patients, as shown by the increased dorsal shift of the nerve among the normal subjects. When the wrist was flexed, the flattening ratios and the cross sectional areas showed no clear trends in either the CTS patients or in the matched normals. However, localized nerve deformation was greater in the normal subjects than in the CTS patients during all flexed-wrist hand activities. The nerve was also more mobile among the normal subjects during all flexed-wrist hand activities. These shifts were statistically significant when the hand was relaxed ($p = 0.023$), and approached significance during both the squeeze grip ($p = 0.089$) and index pinch ($p = 0.095$) activities.

Nerve Appearance During Isometric Loading

Performing an isometrically loaded hand activity tended to slightly decrease the nerve cross-sectional area from the unloaded condition in both the CTS patients and in the matched normals, although these decreases were not statistically significant. There was no clear trend in changes of nerve flattening ratio or in incidence of a nerve dorsal shift associated with hand loading in either the CTS patient or in the normal groups. There was typically a slight increase in the percentage of locally deformed nerve boundary associated with loading in the CTS patients, whereas the matched normals often demonstrated a slight decrease in the percentage of locally deformed nerve boundary upon loading (Table 1). These changes in nerve deformation associated with hand loading may be associated with the increased incidence of a dorsal shift in the normal subjects. Those shifts may have allowed the nerve to move clear of the adjacent flexor tendons responsible for causing localized deformation upon loading.

DISCUSSION

The goal of this study was to quantify local deformations of the median nerve apparent in MR images of the carpal tunnel. Symptomatic CTS patients and matched normal subjects were compared during wrist flexion and isometric hand loading to observe differences in the interactions of the median nerve with its surrounding structures. This work describes a new approach for quantifying localized changes in median nerve shape resulting from interactions with the individual digital flexor tendons and the carpal tunnel boundary. It was evident that there was appreciable interaction between the median nerve and adjacent tendons that resulted in local protrusions of and intrusions into the nerve boundary. These deformations were observed in both subject groups, but surprisingly, there was more localized nerve deformation in the normal subjects than in the CTS patients.

The presence of higher levels of localized deformation in the median nerve of normal subjects was the opposite of our initial hypothesis. However, this finding indicated that the new shape measure was highly sensitive to nerve deformation that was otherwise undetectable using the lower-order traditional shape metrics. Consistent with previous MRI investigations of nerve geometry,[11,14,23] we found slightly larger and slightly flatter nerves in the CTS patient group, although these patients had more regularly shaped nerves with fewer and less pronounced local deformations. The normal nerves, with their smaller cross sectional areas and rounder overall shapes, had more occurrences of small, localized deformations that were detectable only using shape numbers. This may indicate that the median nerve or the immediately adjacent epineural or subsynovial connective tissues of normal subjects are more compliant than in CTS patients, and therefore more able to undergo larger local deformation without a more global change in overall nerve flattening.

In addition to possibly being more compliant, the median nerve in normal subjects also tended to be more mobile than in CTS patients. The increased incidence of a dorsal shift in

the median nerve of normal subjects allowed the nerve to slip past the actively tensed adjacent tendons when the hand was loaded. This greater mobility may account for the reason that there were slight decreases in local deformation among the normal subjects when the hand was loaded, as compared to the relaxed state. The more stationary nerves of the CTS patients may have been responsible for the slight increases in the percentage of locally deformed boundary that resulted when CTS patients performed the isometric loading activities, since the stationary nerve was unable to slip clear of the tensed flexor tendons.

A key finding of this work was the very high variability in nerve deformation within the normal subject group and within the CTS patient group. This high variability limited the identification of statistically conclusive differences between the CTS patient and normal subject groups (Figs. 4, 5). Compounding the challenge in achieving statistical significance, the sample size of 12 matched pairs was reduced for six of the eight scanning conditions, due to insufficient MR image quality. When a CTS patient or their matched normal were performing isometric hand loading, any movement artifact from trying to maintain the isometric load resulted in the inability to analyze that pair's images. In some of the more challenging loading configurations, such as the flat-press with a flexed wrist, there were as few as 6 matched pairs available for analysis. Future studies would benefit not only from a larger number of matched pairs, but also from decreased scanning time to reduce the incidence of motion artifact.

A second limitation of this work was that all of the hand activities were performed in the same order: neutral—relaxed; neutral—flat press; neutral—squeeze grip; neutral—index pinch; flexed—relaxed; flexed—-flat press; flexed—squeeze grip; flexed—index pinch. This was done to expedite the scanning process and to minimize patient fatigue. The prone positioning in the scanner with the arm overhead sometimes resulted in shoulder and back fatigue, and the hand loading activities sometimes resulted in a slight increase in CTS symptoms in some CTS patients. The more fatigued or symptomatic a subject became during scanning, the higher the likelihood of movement artifact degrading the resulting images. Therefore, to ensure the best chance for the subject to provide eight high-quality scans, the most rapid order was always used. This may have resulted in some of the shape measures being influenced by immediately previous activities. However, all subjects were allowed at least 60 s between each scan to relax and rest their hand, providing time for the carpal tunnel tissues to return to their baseline configuration.

The higher degree of localized deformation in the median nerves of normal subjects without a history of CTS was the opposite of the original hypothesis. It was originally anticipated that more frequent and/or more severe local nerve deformations would indicate more severe nerve compression, consistent with more symptoms of CTS. However, the data showed that under identical isometric loads, the nerves of CTS patients tended to be less deformable than the nerves of normal subjects. Certain pathological conditions such as diabetes,[4] Charcot–Marie–Tooth disorder,[19] and glaucoma[18] have been shown to cause substantial increases in nerve stiffness. Therefore, one plausible explanation for less localized deformation in the CTS patients is that the nerve, and/or the subsynovial connective tissue surrounding the nerve is mechanically stiffer than in normal subjects, and thus does not deform as dramatically at locations of direct interaction with neighboring structures. It is also possible that nerve edema, which develops within the nerve after compression[16] and which can increase the endoneurial pressure,[20] may effectively stiffen the median nerve in CTS patients and thus attenuate local deformations that would otherwise result from contact with adjacent tissue structures. This possibility is supported by the frequently noted increase in signal intensity on T2-weighted MRI images of patients with CTS.[1] Based on the present work, a mechanical investigation of median nerve compressive behavior in CTS patients

may provide useful information about changes in nerve behavior associated with CTS pathology.

The localized measure of nerve deformation developed in this work allowed for quantifying the degree to which the median nerve was deformed by adjacent tissue structures. Use of this metric revealed that the median nerve in CTS patients tended to be less locally deformed than in normal subjects, despite being more globally flattened. The potentially increased nerve stiffness and the decreased nerve mobility reported in this work may help explain the nature of the chronic compression associated with CTS symptoms. On MRI, a regularly shaped nerve in the common volar position within the tunnel with a slightly elevated cross sectional area and a slightly flattened aspect ratio would increase the index of suspicion for diagnosis of CTS. It is also important to bear in mind that following carpal tunnel release surgery, the median nerve in CTS patients may not move or behave mechanically in the same way as a normal healthy nerve.

Acknowledgments

We would like to acknowledge Dr. M. Bridget Zimmerman for her help regarding statistics.

References

1. Andreisek G, Crook DW, Burg D, Marincek B, Weishaupt D. Peripheral neuropathies of the median, radial, and ulnar nerves: MR imaging features. Radiographics. 2006; 26(5):1267–1287. [PubMed: 16973765]
2. Bribiesca E. Arithmetic operations among shapes using shape numbers. Pattern Recognit. 1981; 12(2):123.
3. Chan TF, Vese LA. Active contours without edges. IEEE Trans Image Process. 2001; 10(2):266–277. [PubMed: 18249617]
4. Chen RJ, Lin CC, Ju MS. In situ transverse elasticity and blood perfusion change of sciatic nerves in normal and diabetic rats. Clin Biomech (Bristol, Avon). 2010; 25(5):409–414.
5. Girgis WS, Epstein RE. Magnetic resonance imaging of the hand and wrist. Semin Roentgenol. 2000; 35(3):286–296. [PubMed: 10939130]
6. Jablecki CK, Andary MT, So YT, Wilkins DE, Williams FH. Literature review of the usefulness of nerve conduction studies and electromyography for the evaluation of patients with carpal tunnel syndrome. AAEM Quality Assurance Committee. Muscle Nerve. 1993; 16(12):1392–1414. [PubMed: 8232399]
7. Keith MW, Masear V, Chung K, Maupin K, Andary M, Amadio PC, Barth RW, Watters WC III, Goldberg MJ, Haralson RH III, Turkelson CM, Wies JL. Diagnosis of carpal tunnel syndrome. J Am Acad Orthop Surg. 2009; 17(6):389–396. [PubMed: 19474448]
8. Kunze, NM. Master's Thesis. Iowa City, IA: Department of Biomedical Engineering, University of Iowa; 2010. Investigation of local deformation of the median nerve in magnetic resonance images of the carpal tunnel.
9. Kunze NM, Goetz JE, Thedens DR, Baer TE, Lawler EA, Brown TD. Individual flexor tendon identification within the carpal tunnel: a semi-automated analysis method for serial cross-section magnetic resonance images. Orthop Res Rev. 2009; 1:1.
10. Mesgarzadeh M, Schneck CD, Bonakdarpour A. Carpal tunnel: MR imaging. Part I. Normal anatomy. Radiology. 1989; 171(3):743–748. [PubMed: 2717746]
11. Mesgarzadeh M, Schneck CD, Bonakdarpour A, Mitra A, Conaway D. Carpal tunnel: MR imaging. Part II. Carpal tunnel syndrome. Radiology. 1989; 171(3):749–754. [PubMed: 2541464]
12. Middleton WD, Kneeland JB, Kellman GM, Cates JD, Sanger JR, Jesmanowicz A, Froncisz W, Hyde JS. MR imaging of the carpal tunnel: normal anatomy and preliminary findings in the carpal tunnel syndrome. AJR Am J Roentgenol. 1987; 148(2):307–316. [PubMed: 3492109]
13. Mogk JP, Keir PJ. Wrist and carpal tunnel size and shape measurements: effects of posture. Clin Biomech (Bristol, Avon). 2008; 23(9):1112–1120.

14. Monagle K, Dai G, Chu A, Burnham RS, Snyder RE. Quantitative MR imaging of carpal tunnel syndrome. AJR Am J Roentgenol. 1999; 172(6):1581–1586. [PubMed: 10350293]
15. Padua L, LoMonaco M, Gregori B, Valente EM, Padua R, Tonali P. Neurophysiological classification and sensitivity in 500 carpal tunnel syndrome hands. Acta Neurol Scand. 1997; 96(4):211–217. [PubMed: 9325471]
16. Powell HC, Myers RR. Pathology of experimental nerve compression. Lab Invest. 1986; 55(1):91–100. [PubMed: 3724067]
17. Radack DM, Schweitzer ME, Taras J. Carpal tunnel syndrome: are the MR findings a result of population selection bias? AJR Am J Roentgenol. 1997; 169(6):1649–1653. [PubMed: 9393185]
18. Roberts MD I, Sigal A, Liang Y, Burgoyne CF, Downs JC. Changes in the biomechanical response of the optic nerve head in early experimental glaucoma. Invest Ophthalmol Vis Sci. 2010; 51(11): 5675–5684. [PubMed: 20538991]
19. Rosso G, Negreira C, Sotelo JR, Kun A. Myelinating and demyelinating phenotype of Trembler-J mouse (a model of Charcot–Marie–Tooth human disease) analyzed by atomic force microscopy and confocal microscopy. J Mol Recognit. 2012; 25(5):247–255. [PubMed: 22528185]
20. Rydevik B, Nordborg C. Changes in nerve function and nerve fibre structure induced by acute, graded compression. J Neurol Neurosurg Psychiatry. 1980; 43(12):1070– 1082. [PubMed: 7217952]
21. Steinbach LS, Smith DK. MRI of the wrist. Clin Imaging. 2000; 24(5):298–322. [PubMed: 11331161]
22. van Doesburg MHM, Henderson J, Yoshii Y, van der Molen ABM, Cha SS, An KN, Amadio PC. Median nerve deformation in differential finger motions: ultrasonographic comparison of carpal tunnel syndrome patients and healthy controls. J Orthop Res. 2012; 30(4):643–648. [PubMed: 21953849]
23. Weiss KL, Beltran J, Lubbers LM. High-field MR surface-coil imaging of the hand and wrist. Part II. Pathologic correlations and clinical relevance. Radiology. 1986; 160(1):147–152. [PubMed: 3715026]
24. Weiss KL, Beltran J, Shamam OM, Stilla RF, Levey M. High-field MR surface-coil imaging of the hand and wrist. Part I. Normal anatomy. Radiology. 1986; 160(1):143–146. [PubMed: 3715025]
25. Yao L, Gai N. Median nerve cross-sectional area and MRI diffusion characteristics: normative values at the carpal tunnel. Skelet Radiol. 2009; 38:355–361.

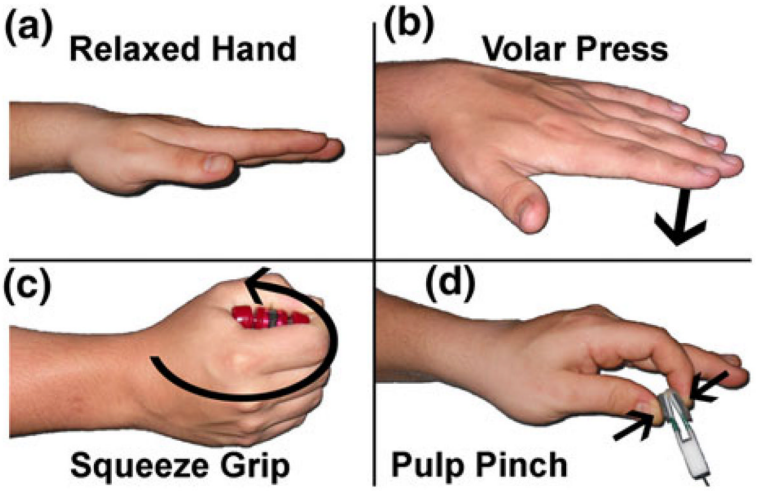

FIGURE 1.

Four isometric loading conditions used during MRI scanning. Subjects were scanned (a) with the hand relaxed, (b) while performing a volar press with all fingers extended, (c) while performing a squeeze grip, and (d) while performing a pulp pinch. Each activity was performed with the wrist in 0 degrees of flexion, and then again with the wrist in 35 degrees of flexion.

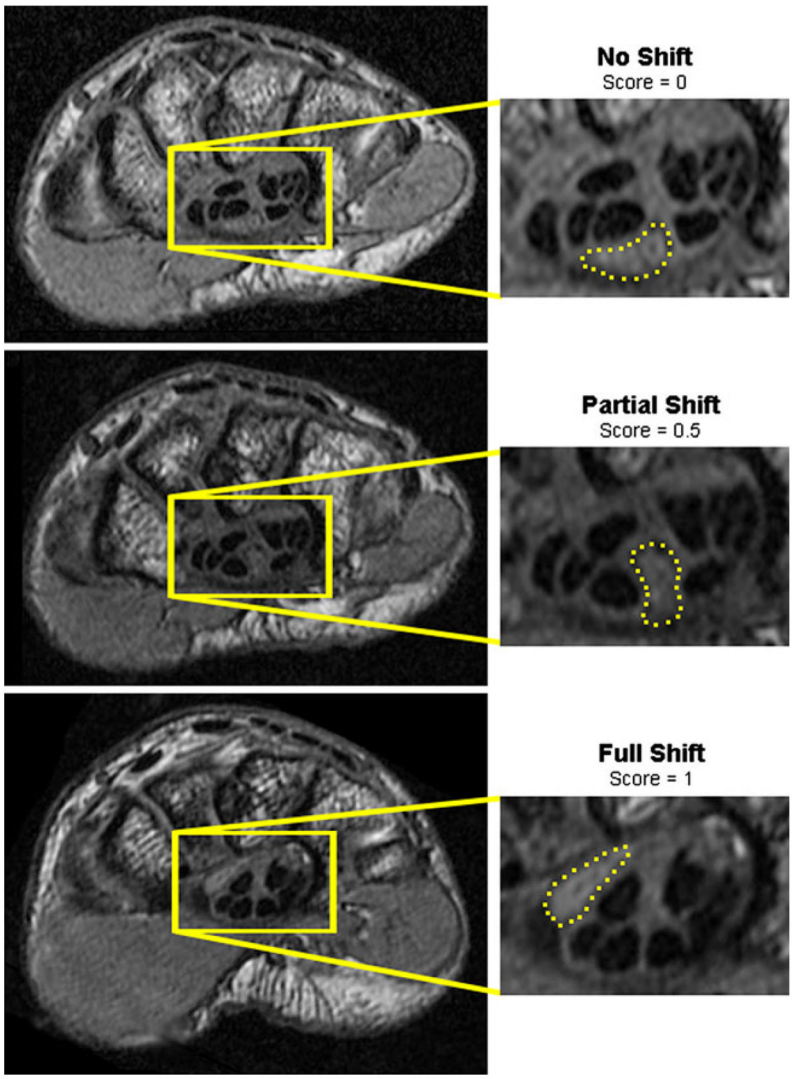

FIGURE 2.

Three positions of the median nerve (dashed outline) in a single patient illustrating the different types of dorsal nerve shifts. When the wrist was in neutral and the hand unloaded (top), the nerve rested on the volar side of the tunnel. When the hand was performing a flat press activity (middle), the nerve partially shifted. When the wrist was flexed and the hand unloaded (bottom), the nerve shifted to the dorsal side of the tunnel.

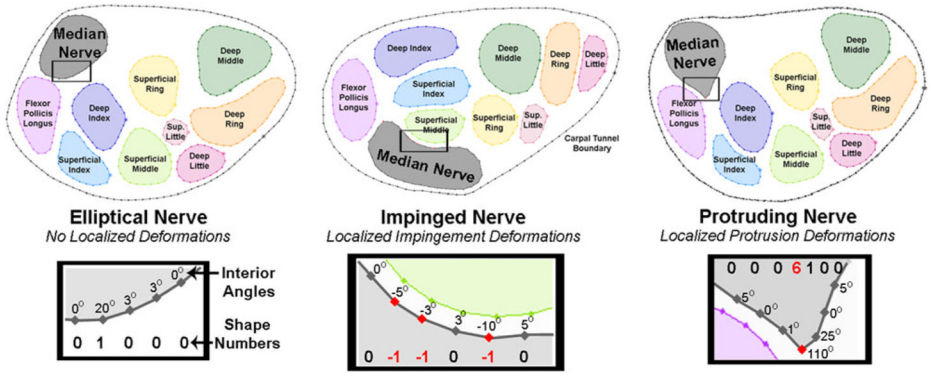

FIGURE 3.

Illustration of different shape numbers calculated from the interior angles of the median nerve boundary. Nerves with smoothly elliptical boundaries had shape numbers ranging from 0 to 2 (left). Nerves being impinged upon by adjacent structures had negative shape numbers in the impinged region (middle). Nerve protrusions were indicated by positive shape numbers greater than those normally found in a smoothly elliptical boundary (i.e., ≥3, which corresponds to ≥60° change in nerve perimeter) (right).

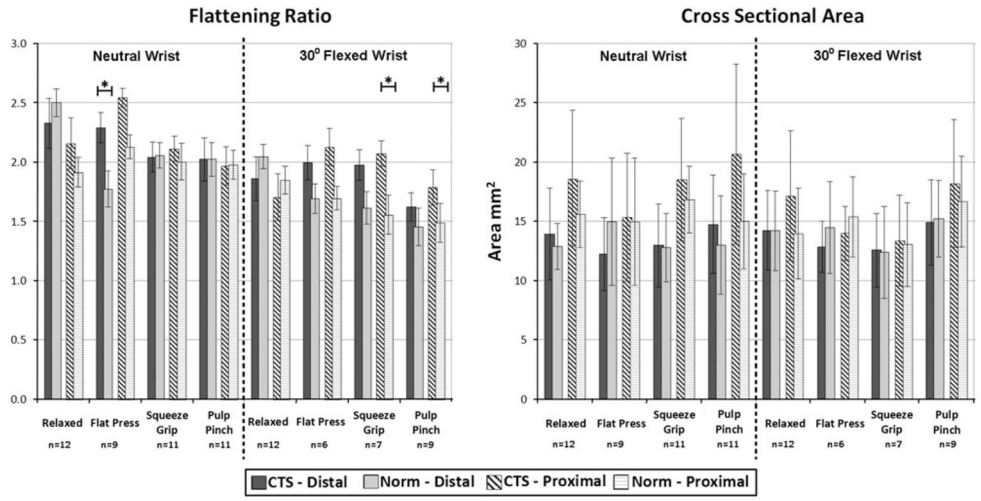

FIGURE 4.

Traditional nerve measures during different isometrically loaded hand activities. The numbers of pairs in each average are indicated under the activity, and SD are shown with the error bars. Cases with fewer than 12 matched pairs resulted from motion artifact preventing analysis of shape metrics in one or more pairs. The solid bars indicate results in the distal part of the tunnel (level of the hook of the hamate), and hashed bars indicate results in the proximal part of the tunnel (level of the pisiform). Activities with statistically significant (p <0.05) differences between CTS patients and normal controls are indicated with an asterisk.

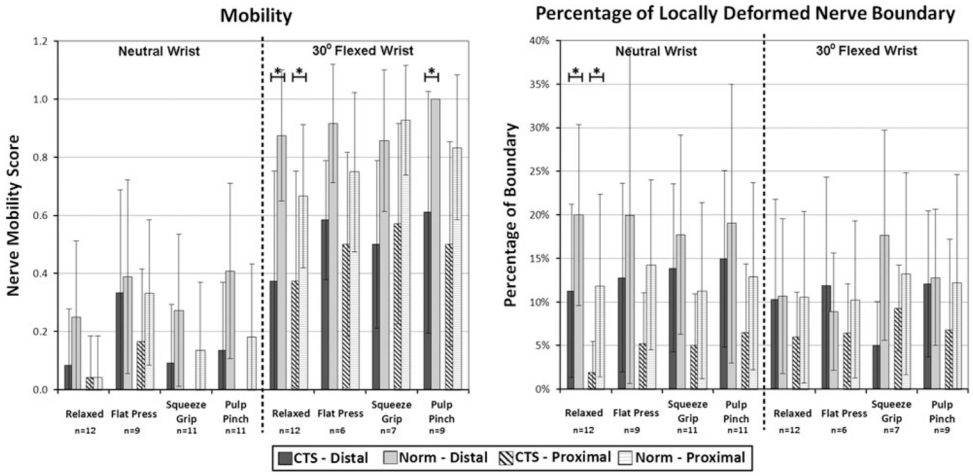

FIGURE 5.

Nerve mobility and new shape measure values during different isometrically loaded hand activities. The numbers of pairs in each average are indicated under the activity, and SD are shown with the error bars. Cases with fewer than 12 matched pairs resulted from motion artifact preventing analysis of shape metrics in one or more pairs. The solid bars indicate results in the distal part of the tunnel (level of the hook of the hamate), and hashed bars indicate results in the proximal part of the tunnel (level of the pisiform). Activities with statistically significant (p <0.05) differences between CTS patients and normal controls are indicated with an asterisk. There was a trend for more nerve mobility and more locally deformed boundary in normal controls (lighter bars), but these results were rarely statistically significant. There was much more nerve mobility with a flexed wrist.

TABLE 1

Changes in nerve shape measures associated with application of each isometric hand load.

	CTS patient				Normal			
	Flattening ratio	**Cross sec. area (mm^2)**	**Mobility (0–l)**	**Boundary deformation**	**Flattening ratio**	**Cross sec. area (mm^2)**	**Mobility (0–1)**	**Boundary deformation**
Distal tunnel								
Neutral Flat press	−0.01 (0.95)	−1.64 (2.95)	0.28 (0.44)	−1% (15%)	−0.67 (1.10)	2.90 (4.29)	0.13 (0.31)	0% (16%)
Neutral Squeeze grip	−0.25 (0.49)	−0.61 (2.24)	0.05 (0.27)	2% (9%)	−0.40 (1.17)	−0.61 (3.13)	0.04 (0.40)	−3% (15%)
Neutral Pulp pinch	−0.11 (0.81)	0.62 (3.38)	0.05 (0.27)	4% (16%)	−0.42 (1.67)	−0.03 (3.97)	0.13 (0.43)	−1% (18%)
Flexed Flat press	0.09 (0.20)	−1.14 (1.76)	0.23 (0.26)	1% (6%)	−0.33 (0.39)	−0.93 (1.55)	0.00 (0.00)	−6% (9%)
Flexed Squeeze grip	0.14 (0.52)	−2.03 (2.96)	0.06 (0.39)	2% (13%)	−0.25 (0.80)	−2.10 (2.29)	−0.10 (0.32)	8% (10%)
Flexed Pulp pinch	−0.32 (0.77)	−0.25 (4.37)	0.15 (0.24)	5% (12%)	−0.47 (0.37)	−0.36 (2.81)	0.05 (0.15)	0% (11%)
Flexion No load	−0.31 (0.90)	0.32 (2.77)	0.29 (0.40)	−1% (12%)	−0.62 (1.04)	1.34 (3.76)	0.63 (0.31)	−9% (14%)
Proximal tunnel								
Neutral Flat press	0.28 (0.44)	−2.52 (3.95)	0.17 (0.25)	4% (6%)	0.27 (0.56)	0.18 (3.90)	0.25 (0.26)	2% (10%)
Neutral Squeeze grip	−0.13 (0.41)	0.40 (3.12)	−0.05 (0.15)	3% (7%)	0.18 (0.52)	0.92 (3.28)	0.08 (0.29)	−1% (14%)
Neutral Pulp pinch	0.05 (0.86)	1.31 (5.84)	−0.05 (0.15)	5% (9%)	0.01 (0.45)	−0.75 (4.28)	0.13 (0.23)	0% (16%)
Flexed Flat press	0.18 (0.80)	−2.21 (4.73)	0.18 (0.25)	−1% (8%)	−0.22 (0.39)	0.03 (1.16)	0.07 (0.19)	1% (10%)
Flexed Squeeze grip	0.09 (0.77)	−2.65 (3.17)	0.05 (0.37)	3% (8%)	−0.09 (0.50)	0.74 (3.12)	0.15 (0.34)	2% (13%)
Flexed Pulp pinch	−0.17 (1.16)	1.38 (5.22)	0.05 (0.28)	1% (9%)	−0.34 (0.52)	1.75 (3.63)	0.14 (0.39)	−1% (12%)
Flexion No load	−0.38 (0.50)	−1.35 (4.99)	0.31 (0.43)	4% (6%)	−0.07 (0.46)	−1.61 (3.17)	0.63 (0.23)	−1% (10%)

*Data expressed as average (SD).

**Decrease of flattening ratio indicates a rounder nerve.